e-Prime - Advances in Electrical Engineering, Electronics and Energy 10 (2024) 100820

Contents lists available at ScienceDirect

e-Prime - Advances in Electrical Engineering, Electronics and Energy

journal homepage: www.elsevier.com/locate/prime

Convolutional neural network approach for fault detection and characterization in medium voltage distribution networks

Atefeh Pour Shafei [a,*], J.Fernando A. Silva [b], J. Monteiro [c]

[a] Electrical Engineering and works at TEPDC (Tehran Electric Power Distribution Company) as a Senior Expert and the Network Fault Analyzer, Building NO.3, Northwest Deputy, Ayatollah Kashani Boulevard, Second Sadeghiyeh Square, Tehran, Iran
[b] INESC-ID, IST, Universidade de Lisboa, Lisbon, Portugal
[c] INESC-ID, Instituto Politécnico de Lisboa, ISEL, Lisbon, Portugal

ARTICLE INFO

Keywords:
Fault detection and characterization
Distribution network
Park transform
Machine learning
Convolutional neural network (CNN)

ABSTRACT

Power outages significantly impact the power industry by disrupting social welfare and economic stability. Still, existing methods for fault detection face challenges due to load and network topology, conditions, and installed equipment. However, recent advances in artificial intelligence (AI) are enabling researchers to create alternative approaches for fault detection and location strategies. Therefore, this paper introduces a novel method for detecting, classifying, and locating faults in power systems through voltage waveform analysis using a convolutional neural network (CNN) integrated with the Piecewise Function Put Together (PFPT) algorithm for fault detection and fault zone localization in a power distribution network. Utilizing Park's transformation, noise reduction PFPT sine fitting, and CNNs, the proposed method distinguishes between 'healthy' and 'faulty' conditions. Simulation results reveal that while the voltage Park's vector time behavior of a healthy system remains stable, it exhibits circular or mixed patterns under faulty conditions. These patterns enable the identification of four types of short circuit faults—single-line-to-ground (LG), line-to-line (LL), line-to-line-to-ground (LLG), and three-line (3L) faults—by analyzing 3D voltage Park's waveforms at network buses. The study validates fault type identification through the observation of rotating Park vectors from sine fitting of time-based voltage waveforms. By converting 3D voltage waveforms into high-resolution images, the method utilizes a CNN for fault recognition, achieving an accuracy of 93.1%. This innovative approach underscores the robustness and precision of combining traditional electrical engineering techniques with modern AI.

1. Introduction

Short circuits in power distribution networks can occur due to a variety of factors, such as unfavorable weather conditions (wind, storms, lightning, dust), equipment malfunctions (including transformers and circuit breakers), cable and transformer winding insulation failures, aging infrastructure, and human mistakes. These faults generate abnormally high currents that may damage equipment. Over time, many techniques have been developed to detect and protect against such faults [1]. A commonly used protection method involves the use of relays. However, while relays can trip during faults, they do not indicate the fault's type or location. This limitation, along with the increasing complexity of power systems, has heightened the demand for accurate and efficient fault classification and location techniques, particularly in distribution grids where the quick restoration of power is crucial. This highlights the importance of a precise fault classification and location system, requiring swift fault analysis, classification, and location to ensure a timely response [2].

In typical distribution networks, faults often cause a drop in bus voltage during the transient spike (known as a voltage sag or dip) and a sharp rise in line current. Voltage sags are characterized by a temporary decrease of more than 10 percent in voltage during the fault time. The extent and duration of this voltage dip are influenced by factors such as system impedance, fault location, fault duration, and the protective devices in place [3]. Fault current is divided between grounding electrodes and medium voltage (MV) cable sheaths, largely determined by the line impedances of the power distribution network and the type of short circuit [4]. Therefore, a simple approach to detect and locate faults could involve measuring the depths of voltage sags and the corresponding fault currents. Further research has soon devised several

* Corresponding author.
E-mail addresses: a.pourshafie@gmail.com (A.P. Shafei), fernando.alves@tecnico.ulisboa.pt (J.FernandoA. Silva), jmonteiro@deea.isel.ipl.pt (J. Monteiro).

https://doi.org/10.1016/j.prime.2024.100820
Received 11 April 2024; Received in revised form 22 September 2024; Accepted 16 October 2024
Available online 18 October 2024

methods for fault detection, classification, and location, considering factors such as features, inputs, complexity, systems used and outcomes [5]. Thus, now fault detection techniques include impedance-based, knowledge-based, and hybrid approaches.

Impedance-based algorithms, although established since the early stages of power systems, are hampered by load conditions, high grounding resistance, and series capacitor banks, particularly in transmission lines [6]. These drawbacks have led to studies on traveling-wave fault location (TWFL) methods since 1931, especially for transmission lines [7]. However, large-scale applications have only emerged in recent decades due to advances in the technology of analog-to-digital converters (ADCs) used by digital fault recorders (DFRs) and digital relays. In general, TWFL (Traveling Wave Fault Location) methods provide greater accuracy than impedance-based approaches, as their accuracy relies solely on the sampling rates of the Data Acquisition (DAQ) system and time synchronization, despite the need for specialized equipment [6]. Nevertheless, TWFL methods encounter challenges when implemented in distribution networks due to factors such as:

- Non-homogeneity of lines (unbalances)
- Existence of laterals
- Required measurements and the sparsity of monitoring devices
- Uncertainty of network data [8]
- Integration of distributed intermittent generation and micro-grids, which can operate in grid-connected or stand-alone modes, complicating fault location [9]
- Bi-directional power flow, where multiple sources of potential fault current make detection and fault location more complex, potentially rendering auto re-closure unsuccessful due to continuous current feeding by distributed generators [10]
- Presence of sensors, IoT, controllers, and information/communications facilities along the main feeder and laterals [11]
- Limited fault currents due to power electronics, which are often used to connect renewable generation to the power grid [12]

Recent advances in signal processing, artificial intelligence (AI), and machine learning (ML) are enabling researchers to explore new approaches to traditional fault detection and location strategies. The general strengths and weaknesses of various AI and ML-based algorithms, such as convolutional neural networks (CNN), are well understood, allowing researchers to make informed choices in selecting and applying these methods for fault detection. As a result, new hybrid approaches have emerged, combining signal processing techniques with AI. In particular, the Adaptive Neuro-Fuzzy Inference System (ANFIS) has shown notable accuracy [13]. However, comparing fault detection methods remains difficult due to the unique conditions under which they are tested, making it challenging to determine a universally reliable and cost-effective solution [14].

Park's dq0 transformation is a signal-processing technique used in electrical engineering and power systems analysis to streamline the analysis and control of three-phase electrical systems. It allows for simultaneous monitoring of faults across all system phases by processing voltage or current waveform samples from each phase in a real-time, eliminating the need to store previous waveform samples in a buffer [6]. The dq0 transform generates a rotating reference frame in synchronism with voltage and current phasors at the power frequency ω, which can also detect voltage or current imbalances due to faults [6]. The rotating reference frame can be aligned with the instantaneous position of the three-phase system magnetic field or to another useful position. The generated signals help analyze and control electric machines and inverters more effectively [15]. Park's phasors time behavior generates patterns that can be classified as 'healthy' or 'faulty' conditions [16]. By comparing the patterns of Park's phasors in each phase, faults in distribution lines can be diagnosed.

While most fault diagnosis papers use Park's transformation of current samples during fault conditions for detection, this paper utilizes

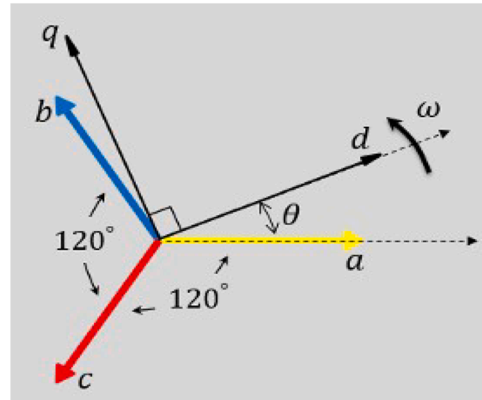

Fig. 1. dq0 application as a transient detection technique [19].

Park's transformation on voltage samples because voltage sensors are often easier to implement and maintain in a distribution network compared to current sensors. Voltage sensors also outnumber current sensors in distribution networks. Moreover, voltage deviations during faults are often more delimited and easier to detect compared to current changes. This makes voltage-based fault detection more sensitive and potentially faster [17]. Therefore, this paper proposes a fault detection hybrid approach, using CNNs and Park's transformation for voltage samples with a sine-fitting algorithm.

The main innovations in this paper include a unique noise-reducing procedure using sine-fitting methods averaging the four nearest samples to provide noise-free voltage values to the dq0 transform for real-time fault monitoring significantly enhancing detection efficiency and speed, without the needed buffer storage of moving average filters. The proposed method provides trustworthy comparisons with actual voltage measurements ensuring the accuracy of CNN fault detection. The proposed CNN fault detection technique operates effectively without the need of complex communication networks, requiring only data communication at each bus to measure and transmit voltages. This may help reduce infrastructure complexity and maintenance costs.

The paper is organized as follows: first, Section 2 describes the training data preparation. Then, in Section 3 the artificial intelligence method is proposed. Next, Section 4 describes a case study to evaluate the proposed method. Section 5 deals with the CNN Fitting Method, while Section 6 presents the machine learning outputs for the proposed method. Before the conclusion, Section 7 compares the accuracy of the proposed method with state-of-the-art existing methods.

2. Training data preparation

2.1. Park's transformation

The dq0 transformation is a mathematical technique used in the fields of power systems modeling and control. It transforms the abc coordinates to a new coordinate system (dq0) that rotates at the same frequency as the electrical machine or system under consideration [18]. The voltage waveform at each sampling time can be written in terms of $V = V_m \cos(\omega t + \Theta_i)$, where V_m is the amplitude value, ω is the angular frequency, t is the time, and Θ_i is the phase angle, representing the shift of the waveform along the time axis, regarding a reference.

Fig. 1 and Eq. (1) show the dq0 vectors in terms of the three-phase system voltages, abc, where θ is the electrical angle in radians $\theta = \omega t + \theta_0$, being θ_0 usually selected to maximize the d component being the q component usually close to zero. Vector a, b, and c represent the three-phase quantities, while dq0 represents the direct (d), quadrature (q), and zero (0) components of Park transformation.

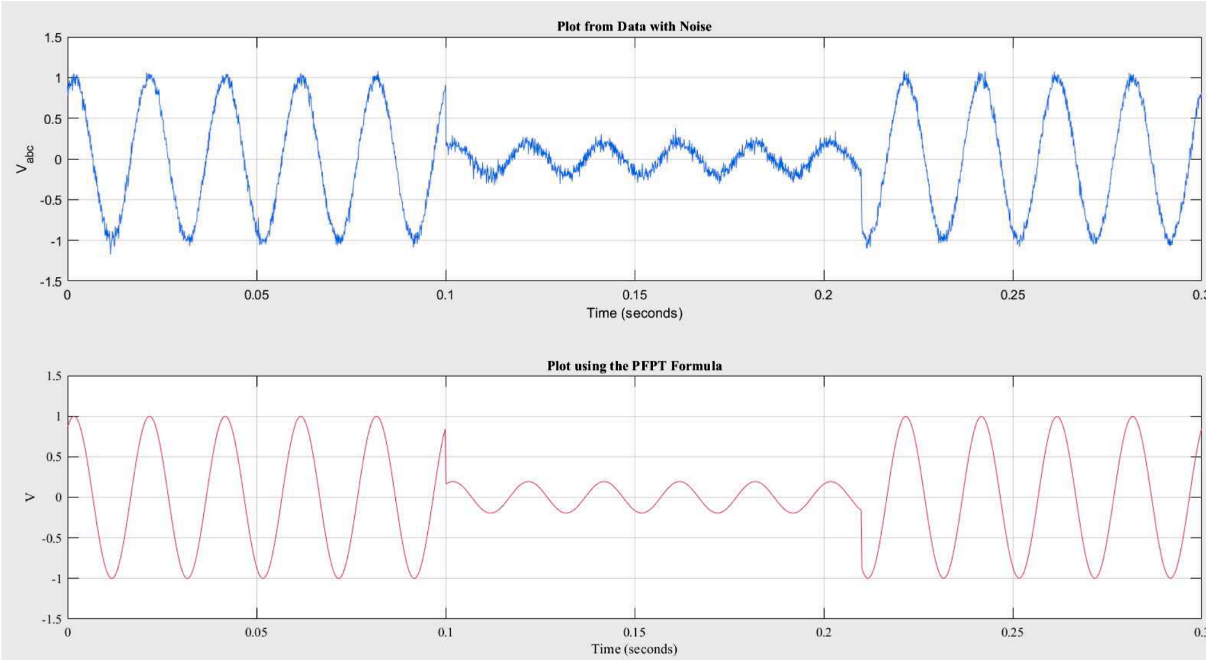

Fig. 2. The plot of a three-phase voltage noisy waveform with a fault, and after using a sine-fitting algorithm; Upper graph: Voltage samples with noise; Bottom graph: Plot using PFPT showing noise reduction.

$$\begin{bmatrix} d \\ q \\ 0 \end{bmatrix} = \frac{2}{3}\begin{bmatrix} \sin(\theta) & \sin\left(\theta - \frac{2\pi}{3}\right) & \sin\left(\theta + \frac{2\pi}{3}\right) \\ \cos(\theta) & \cos\left(\theta - \frac{2\pi}{3}\right) & \cos\left(\theta + \frac{2\pi}{3}\right) \\ \frac{1}{2} & \frac{1}{2} & \frac{1}{2} \end{bmatrix}\begin{bmatrix} a \\ b \\ c \end{bmatrix} \tag{1}$$

2.2. Noise reduction sinusoidal fitting method

During a fault, such as a short circuit, unbalanced currents flow through the system. These currents passing through the line impedance cause voltage drops due to the resistance of the lines and other elements of the system. The voltage values can be sampled and digitized for further processing.

The Park transformation over time can be represented in high-quality images that are used to train a convolutional neural network (CNN) to classify each image. In image classification methods, validation of results is a crucial step to ensure the accuracy and reliability of the identified faults. To achieve this in the presence of noise a sine-fitting algorithm is used to accurately estimate a digitized sinusoidal signal's parameters (V_m amplitude, phase, frequency, and DC component). The extraction of the sine wave parameters is non-iterative if the frequency of the signals is known beforehand. Therefore, this paper uses the three-parameter (V_m amplitude, phase, DC component) sine fitting with the known frequency [19] which is a faster solution compared to iterative solutions. Subsequently, this value is compared to the largest circular magnitude in the Park transform vectors corresponding to the fault event. If these two approaches corroborate each other, it indicates the correctness of the proposed algorithm.

In this study, values of V_m just after the fault occurrence will be calculated using the sine fitting method [19] and the Piecewise Function Put Together (PFPT) formula that essentially combines two or three sine functions with different amplitudes [20]:

The piecewise function $f_{pw}(x)$ as represented in (2) is:

$$f_{pw}(x) = \left\{ \begin{array}{c} f_1(\mathrm{x})\ x \le x_a \\ f_2(\mathrm{x})\ x_a < x \le x_b \\ f_3(\mathrm{x})\ x_b < x \end{array} \right\} \tag{2}$$

Where x is the independent variable, $f_1(x)$, $f_2(x)$ and $f_3(x)$ are the piecewise sine functions, and x_a and x_b with $x_a < x_b$ are the points at which the function transitions.

In this paper, a Heaviside-based formula, referred to as the Piecewise Function Put Together (PFPT) formula, is used as shown in (3):

$$f_{pw}(x) = f_1(x) + [f_2(x) - f_1(x)]H(x - x_a) + [f_3(x) - f_2(x)]\mathrm{H}(x - x_b) \tag{3}$$

In (2), the first term represents $f_1(x)$ throughout the x range. The Heaviside function $H(x - x_a)$ in formula (3) activates the second term $[f_2(x) - f_1(x)]$ when x is greater than or equal to x_a, and the third term $[f_3(x) - f_2(x)]$ when x is greater than or equal to x_b, allowing the piecewise function to transition smoothly between $f_1(x)$, $f_2(x)$, and $f_3(x)$ at specified points x_a and x_b. The second term in (3) is activated by the Heaviside step function when $x \ge x_a$, plotting $f_2(x)$, and canceling out $f_1(x)$ from x_a onwards. Upon reaching x_b, the Heaviside function triggers the 3rd term, plotting $f_3(x)$ and canceling out $f_2(x)$ from x_b onwards.

The upper image in Fig. 2 shows the plot of Vabc from normalized noise affected data, while the lower image shows the results of using (3) formulation on an average of four nearest samples to find the Sin wave time-based function using the sinusoidal fitting curve algorithm. This result proves the most significant advantage of using the PFPT approach, which is the noise reduction capability, making it a performing choice in noisy environments. The "Plot from Data with Noise" in Fig. 2 shows the voltage containing noise. In contrast, the "Plot using the PFPT Formula with Noise Reduction" represents how this method mitigates noise, resulting in a much clearer signal. As evidenced in Fig. 2, the voltage amplitude obtained through the sine fitting method can be used to identify the faulty zone. It can be seen from both graphs of Fig. 2 that a fault occurred in $t = 0.1$ s and was then cleared at $t = 0.2$ s.

Therefore, the voltage V_m amplitude obtained through the sine fitting method can be utilized to identify the faulty zone, enhancing fault detection by more effectively highlighting transient characteristics. This approach also improves validation by minimizing noise and measurement errors. Overall, the PFPT plot offers a clearer and more reliable tool for analyzing voltage waveforms and identifying faults in power distribution networks.

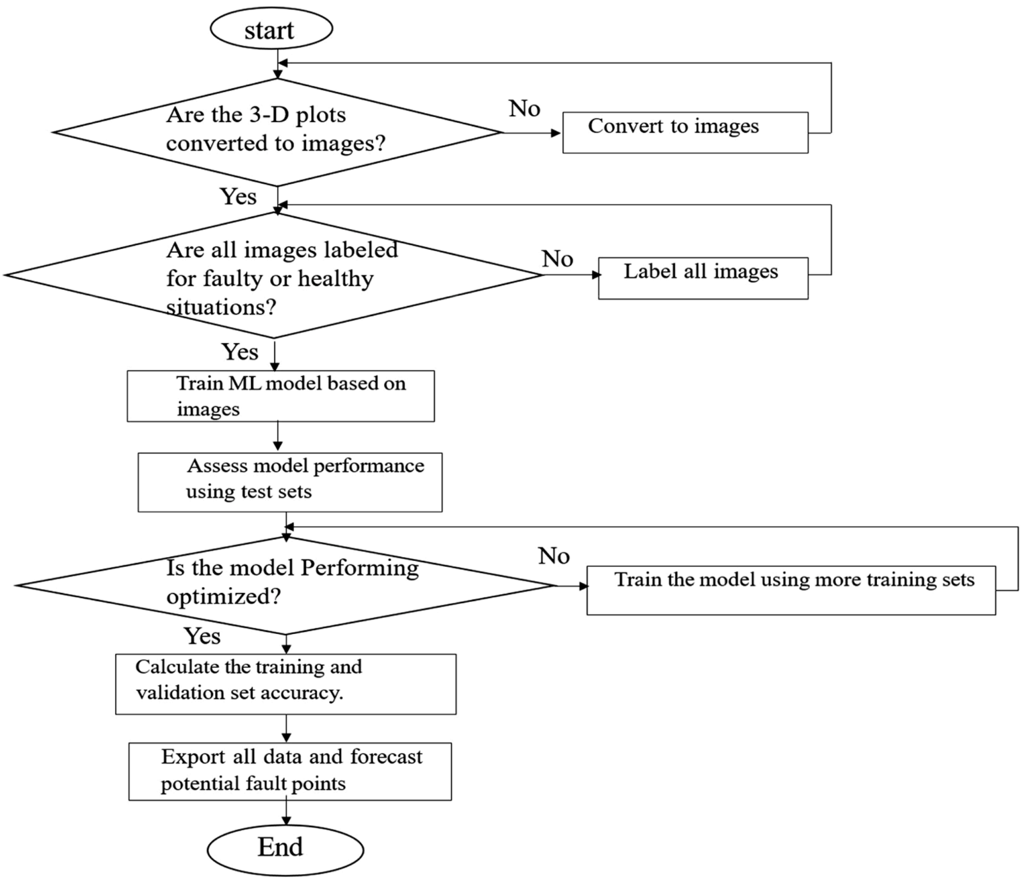

Fig. 3. Flow chart of training model.

3. Proposed artificial intelligence method

The fault detection proposed approach uses pattern recognition and classification CNNs, applied to images created using Park's transformation of noise-canceling sinusoidal fitted voltage values. This approach includes four steps as follows:

1. Fault Creation and Data Acquisition Faults, including single-line-to-ground (LG), line-to-line (LL), line-to-line-to-ground (LLG), and three-line faults (3L), are deliberately forced in the busses of the electrical distribution network under study, using computer simulations. The dq0 graphs of voltages and currents are recorded using the PLL phase ($\omega t+ \theta_0$), with disturbances evident in the d and q components. The circles' size in the Park vectors of normalized voltages at each bus determines the fault type and the faulty bus.
2. Validation. Through noise reduction sinusoidal fitting time-based voltages are evaluated using the sinusoidal fitting method and noise reduction to validate the outcomes of the voltage Park's graph analysis. Different short-circuit faults are analyzed in all buses, and the circles visually represent the transitional regime during fault occurrences.
3. Analysis of Park Circles pre and post-fault. The analysis of Park Circles involves an assessment of the electrical parameters of the distribution network. This step encompasses four key sub-steps:
   3.1. Event Data Collection
   - Gather data on the fault event, specifying fault type, location, and occurrence time.
   - Collect information on distribution network details, including topology, line parameters, and transformer data.

   3.2 Conversion to Park Coordinates
   - After noise reduction sinusoidal fitting, convert three-phase voltage quantities to the rotating reference frame as Park coordinates (abc to dq0).

   3.3 Analyze Park Circles
   - Examine the behavior of rotating vectors in Park coordinates, identifying specific patterns such as oscillations or distortion after a fault.
   - Identify fault characteristics through observations of the behavior of Park circles.
   - Utilize information gathered from Park circles to estimate the fault location within the distribution network.
4. Convert the park circles output to high-quality images to train a convolutional neural network (CNN). Fig. 3 shows this paper's flowchart of the applied machine learning procedure.

To identify the fault types, the voltage waveforms over the fault time are transformed into high-quality images representing d,q transformed space-time trajectories. This process involves converting the 3D voltages into images that visually represent the behavior of the Park vectors under different fault conditions. Each fault type has its own typical image which can be considered as the fault signature pattern. The images are then processed using a convolutional neural network (CNN). The CNN is trained to build criteria to recognize the patterns corresponding to each type of fault by analyzing the shapes, sizes, and colors of the Park vectors in the images. This method utilizes the image classification capabilities of the CNN to accurately detect and classify the faults based on the visual features extracted from the transformed waveforms. The above steps can be used to train another CNN to detect faults in similar distribution networks.

The CNN Training for Image Classification approach through Data Preprocessing would be as follows:

Table 1
Test System Data.

Data	Value	Unit
S_n	10	MVA
V_n	20	kV
f	50	Hz
$Z_1=(R+jX)$	0.0810+j0.0613	$\Omega.km^{-1}$
B_1	76.4474	$\mu S.km^{-1}$
$Z_0=(R+jX)$	0.1668+j0.1333	$\Omega.km^{-1}$
Load No.1 (L_1)	90	kVA
Load No.2 (L_2)	464	kVA
Load No.3 (L_3)	360	kVA
Load No.4 (L_4)	1890	kVA
Load No.5 (L_5)	180	kVA
Load No.6 (L_6)	1750	kVA
Load No.7 (L_7)	643	kVA
Load No.8 (L_8)	1460	kVA

1. **Data Preprocessing**: Effective preprocessing steps, including data augmentation and normalization, significantly contribute to the artificial intelligence method's performance, enhancing its generalization ability across diverse input variations. Image normalization is a crucial preprocessing step that involves adjusting the pixel values of an image to a standardized scale, typically between 0 and 1. This process enhances the model's stability and convergence during training by ensuring that input features are on a consistent scale. In the context of RGB images, normalization often includes dividing the pixel values by 256, contributing to improved convergence and generalization across diverse datasets.
2. **Hyperparameter Optimization:** The systematic exploration of hyperparameters, such as dropout rate, learning rate, and epochs, underscores the importance of identifying an optimal configuration. This approach enhances the model's ability to generalize effectively to unseen data.
3. **Model Architecture:** The model strikes a balance between complexity and interpretability, making it suitable for image classification tasks. The proposed model architecture incorporates two convolutional layers followed by batch normalization. This streamlined neural network structure indicates efficacy for diverse computer vision applications.
4. **Optimization Algorithm:** The Adam optimizer, combined with categorical cross-entropy loss, proves effective for training the CNN model. The adaptive learning rate and optimization updates contribute to efficient convergence.

4. Case study

This case study examines a real 20 kV distribution feeder in the Tehran Electric Power Distribution Company. The data on line types (underground or overhead), impedances, medium voltage loads, 63/20 kV transformer data, and the snubber circuit for mitigating faults were collected from a real 20 kV industrial feeder in Tehran city, derived from the SCADA system of the Tehran Electric Power Distribution Company. Table 1 shows the essential parameters for performing power system studies and simulations of the sample network, shown in Fig. 4, which are the power rating and voltage of the system, as well as series impedance, shunt admittance, and zero sequence impedance.

Fig. 4 shows the schematic of the distribution network under study. It consists of a radial medium voltage industrial distribution feeder. The network is divided into four zones with about 200 m each. It should be noted that each zone contains of at least one bus. Although the data used for CNN training is simulated, it closely replicates real-world conditions and parameters to ensure the accuracy and reliability of the proposed method.

Fig. 5 shows the three-dimensional Park diagrams before and after different fault types occurred in the case study network. Without faults, it shows almost straight lines as the normalized direct and quadrature voltages are nearly constant over time (Fig. 5a).

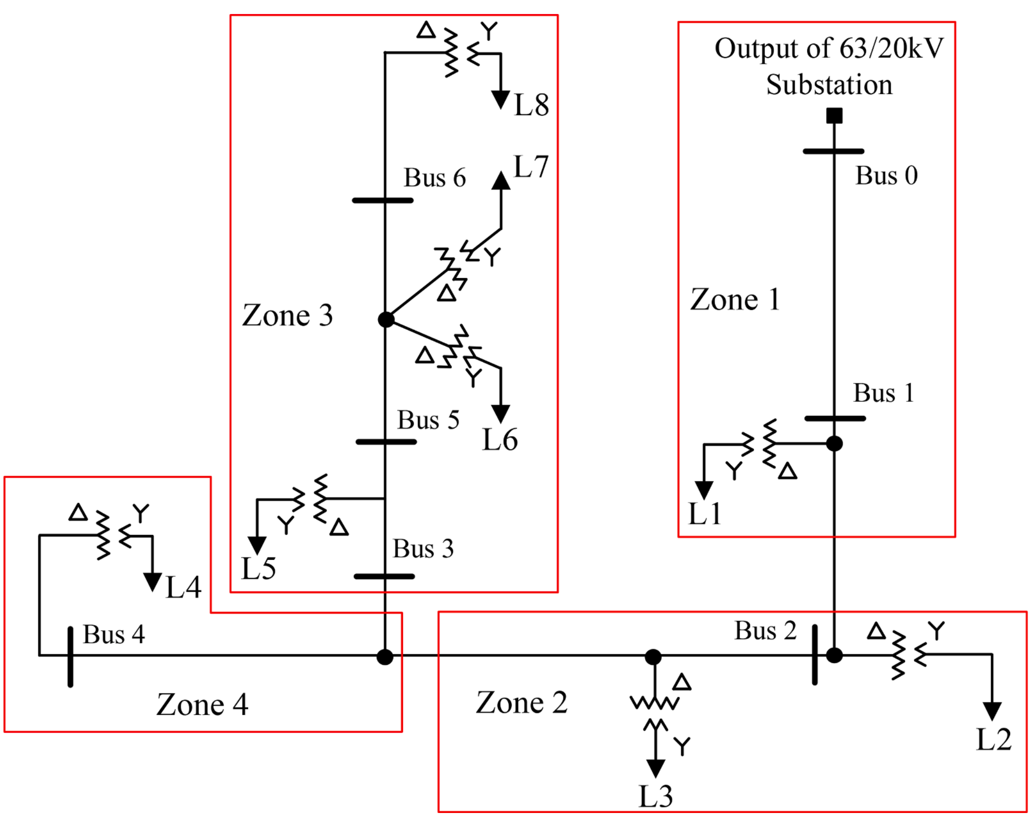

Fig. 4. Diagram of the distribution network under test (existing 20 kV distribution feeder).

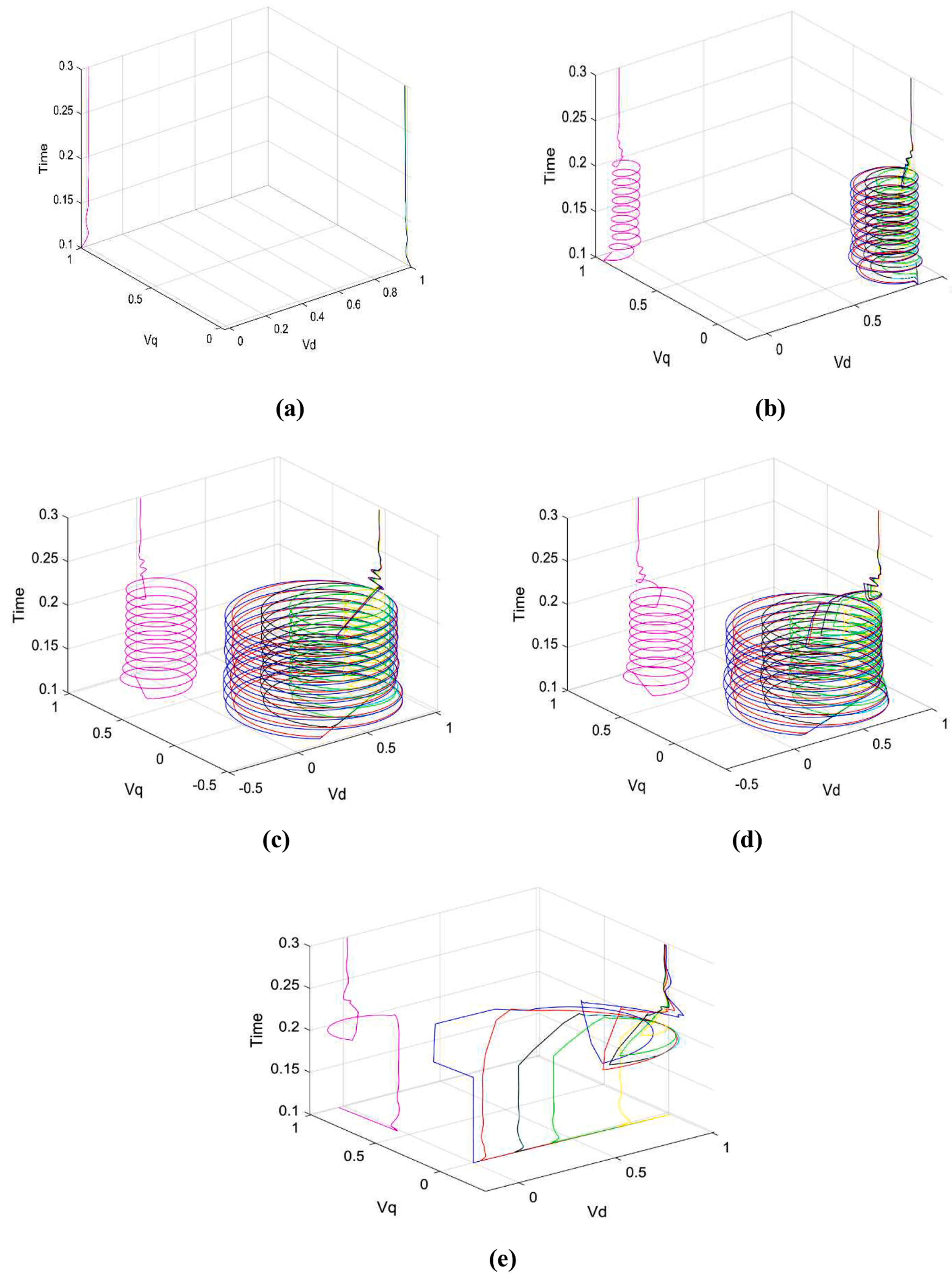

Fig. 5. Three-dimensional representation of voltage Park transforms at Bus No. 6: a) before fault b) after LG fault c) after LL fault d) after LLG fault e) after 3 L fault.

This constant time behavior will disappear, turning to rotating circle trajectories, after LG faults (Fig. 5b), where the direct voltage decreases slightly, then rotates in small circles and nears the initial value after the LG fault, while the quadrature voltage decreases, rotates in small circles and stays lower than the pre-fault value. After LL fault (Fig. 5c), the direct voltage decreases significantly, then rotates in large circles and does not reach the pre-fault value after the LL fault, while the quadrature voltage decreases moderately, rotates in medium diameter circles and stays significantly lower than the pre-fault value. After LLG fault (Fig. 5d) the direct voltage decreases significantly, then rotates in medium/large circles and does not reach the pre-fault value after the LLG fault, while the quadrature voltage decreases significantly, rotates in small to medium diameter circles and stays significantly lower than the pre-fault value. After 3 L fault (Fig. 5e) the direct voltage decreases strongly, stays low and rotates in medium/large circles just after the 3 L fault clears, while the quadrature voltage lowers significantly, stays low during the fault and just rotates after the 3 L fault clears.

Table 2
The Training Data for Zone 1.

Short Circuit Type /Fault Resistance:0.001Ω		3L		LLG		LL		LG	
Zone No.	**Bus No.**	**Biggest circular sectors**	**Bus No MinValue of V_m**	**Biggest Park Circle**	**Bus No MinValue of V_m**	**Biggest Park Circle**	**Bus No MinValue of V_m**	**Biggest Park Circle**	**Bus No MinValue of V_m**
Zone 1	**0**	Yellow (Bus0)	0 to 6 0.0695	Yellow (Bus0)	0 to 6 0.08707	Yellow (Bus0)	0 to 6 0.08708	Yellow (Bus0)	0 to 6 0.8723
	1	Magenta (Bus1)	1 to 6 0.0736	Magenta (Bus1)	1 to 6 0.0851	Magenta (Bus1)	1 to 6 0.09205	Magenta (Bus1)	1 to 6 0.7966

Table 3
The Training Data for Zone 2.

Short Circuit Type/Fault Resistance: 0.001 Ω		3L		LLG		LL		LG	
Zone No.	**Bus No.**	**Biggest circular sectors**	**Bus No MinValue of V_m**	**Biggest Park Circle**	**Bus No MinValue of V_m**	**Biggest Park Circle**	**Bus No MinValue of V_m**	**Biggest Park Circle**	**Bus No MinValue of V_m**
Zone 2	**2**	Green (Bus2)	2 to 6 0.0743	Green (Bus2)	2 to 6 0.08277	Green (Bus2)	2 to 6 0.09291	Green (Bus2)	2 to 6 0.7805

Table 4
The Training Data for Zone3.

Short Circuit Type/Fault Resistance: 0.001 Ω		3L		LLG		LL		LG	
Zone No.	**Bus No.**	**Biggest circular sectors**	**Bus No MinValue of V_m**	**Biggest Park Circle**	**Bus No MinValue of V_m**	**Biggest Park Circle**	**Bus No MinValue of V_m**	**Biggest Park Circle**	**Bus No MinValue of V_m**
Zone 3	**3**	Cyan (Bus3)	3 to 6 0.0748	Cyan (Bus3)	3 to 6 0.0806	Cyan (Bus3)	3 to 6 0.001107	Cyan (Bus3)	3 to 6 0.7657
	5	Red (Bus5)	5,6 0.0752	Red (Bus5)	5,6 0.07878	Red (Bus5)	5,6 8.8753e-04	Red (Bus5)	5,6 0.7599
	6	Blue (Bus6)	6 0.0756	Blue (Bus6)	6 0.07892	Blue (Bus6)	6 8.9693e-04	Blue (Bus6)	6 0.7578

5. The CNN fitting method

Based on the case study, there are 56 diagrams for all fault types, i.e., LG, LL, LLG, and 3L. In the training sets a fault resistance $R = 0.001\Omega$ was considered, while fault resistances of 0.01Ω and 0.1Ω were used to create sets of validation images. This includes 28 diagrams for each fault type occurring near the buses and 28 diagrams for locating each fault type between buses. In other words, there are 7 diagrams for each fault type where the fault is located along the network lines. For example, LG faults occur between bus 0 and bus 1, between bus 1 and bus 2, and so on. This situation is repeated for LL, LLG, and 3 L fault types.

It is expected that because the highest load current passes through bus 1 and bus 2, respectively, the highest overcurrent due to a three-phase short circuit is observed in buses 1 and 2, to facilitate effective fault diagnosis, emphasis has been placed on scrutinizing voltage Park's diagrams. Notably, the decision to prioritize voltage Park transforms over current analysis is that, across various fault scenarios, the Park vectors of current in bus 1 far exceed those in other buses. This deliberate focus on voltage-related information not only aids in pinpointing the fault's location but also contributes valuable insights into discerning the specific type of fault encountered. This analytical strategy enhances the accuracy and efficiency of the fault diagnosis methodology, contributing to a more robust and reliable assessment of power system disturbances. The fitting functions for deep learning are the diameter of the Park's circles and the minimum value of V_m just after the fault occurs at $t = 0.1$ s.

Table 5
The Training Data for Zone 4.

Short Circuit Type/Fault Resistance: 0.001 Ω		3L		LLG		LL		LG	
Zone No.	**Bus No.**	**Biggest circular sectors**	**Bus No MinValue of V_m**	**Biggest Park Circle**	**Bus No MinValue of V_m**	**Biggest Park Circle**	**Bus No MinValue of V_m**	**Biggest Park Circle**	**Bus No MinValue of V_m**
Zone 4	**4**	Black (Bus4)	4 0.0756	Black (Bus4)	4 0.07981	Black (Bus4)	4 9.3790e-04	Black (Bus4)	4 0.7591

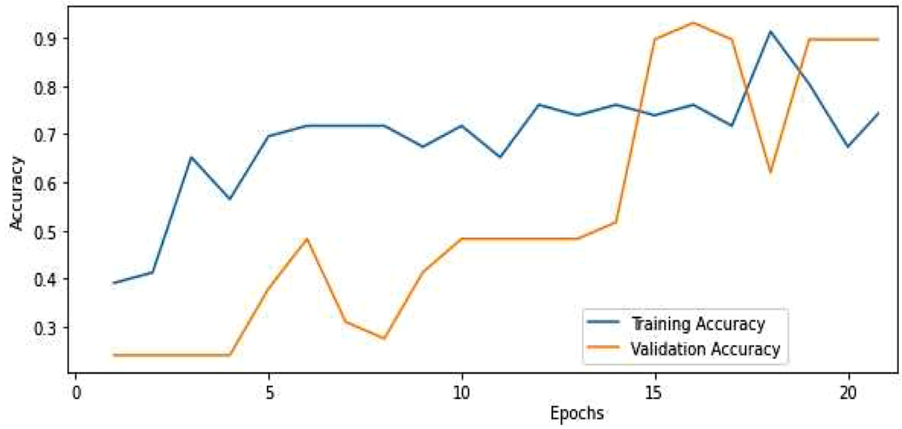

Fig. 6. The progression of training and validation accuracy.

It should be noted that in the case of 3 L faults, instead of having Park circles, a combination of line and circular sectors is observed. Therefore, instead of the diameter of the circle, the radius of the circular sector can be measured after removing the fault at the $t = 0.2$ s as shown in the right side of Fig. 5(e). Tables 2-5 show CNN's primary training data with a fault resistance of 0.001 Ω.

Using the simulation results, i.e., 3-D plots like Fig. 5, firstly, the output data or mat files are converted to high-resolution pictures (Tables 3-5).

A training method with convolutional layers and Sequential Methodology was proposed in 2018 using a fully sequential methodology to construct and train extremely deep convolutional neural networks [21]. The CNN architecture, labeled "sequential_64," encompasses convolutional and fully connected layers. These layers introduce non-linearities through activation functions and prevent overfitting with dropout layers.

In the context of this study, the conversion of output data or ".mat" files into high-resolution images is a critical step for subsequent analysis [22]. The resolution is defined as the pixel density of an image and Dots Per Inch (DPI) as the number of dots per inch when printed. The trade-off between resolution and file size was carefully considered, recognizing that higher-resolution images contain more information but may result in larger file sizes. During the conversion process, meticulous attention is paid to image processing techniques, including interpolation or scaling, to achieve the desired DPI of 2000. The resulting images are then classified based on criteria such as curve diameter and color, contributing to the preparation of a diverse and well-classified image database for algorithm training. The algorithm relies on features extracted from these images, specifically focusing on curve diameter and color. It is observed that when image quality drops below 2000 DPI, accuracy decreases, and conversely when increased to 3000 DPI, accuracy improves. However, it is acknowledged that higher DPI comes at the cost of increased simulation time, prompting a nuanced consideration of the trade-offs between image quality, algorithm accuracy, and computational efficiency.

Next, the image files are classified according to their types. A database containing various and classified images is prepared and delivered to the processing algorithm. Then, based on the features provided to the algorithm, which are based on the diameter and color of the curves, the algorithm makes some guesses and indicates that these nodes are more likely to be in faulty situations. In the end, the image code converts them into a data series, and the deep learning algorithm processes them.

6. Machine learning

In this study, Park's transformation is synergistically integrated with a noise reduction algorithm, image creation and CNNs to enhance the fault diagnostic capabilities of power systems. Following the flowchart of Fig. 3, after the preliminary step of transforming all 3-D plots into high-quality 3-D images with a resolution of 2000 dpi, the machine-learning procedure analyses all the images at the inputs of a CNN model, named "sequential_64″. It consists of two convolutional layers followed by batch normalization and max-pooling, leading to a densely connected layer with 256 neurons.

To determine the optimal values for the number of epochs, learning rate, and drop-out rate, a comprehensive hyperparameter tuning experiment was conducted. Employing a grid search methodology, the model was trained using various combinations of hyperparameters, and its performance was subsequently assessed on the validation set. This involved exploring diverse combinations of epochs and learning rates, as well as drop-out rates. The outcome of this experiment is the identification of the best validation accuracy along with the corresponding set of hyperparameters, providing valuable insights into the configuration that yields optimal model performance. The best results were obtained using a dropout rate of 0.2 to mitigate overfitting. The model is trained for 22 epochs using a learning rate of 0.0001.

The CNN model architecture is presented as follows:

- Input: Image data
- Convolutional Layers: Two layers with 32 and 64 filters, respectively
- Batch Normalization: Applied after each convolutional layer.
- Max-Pooling: Reduces spatial dimensions.
- Dense Layer: 256 neurons
- Dropout: Rate of 0.2
- Output Layer: 5 neurons for multi-class classification.

It should be noted that the carefully chosen hyperparameters and architecture contribute to the model's effectiveness in learning complex features from the input data.

In this step, a non-labeled image is introduced, deliberately excluded from both the training and validation sets, by strategically relocating the fault occurrence between two buses. Training and validation sets for the neural network were generated by varying the fault resistance (0.001 Ω, 0.01 Ω, and 0.1 Ω).

This unique data usage challenges the neural network to adapt it to a previously unseen scenario. Fig. 6 visually depicts the iterative process of adjusting the weights in the neural network architecture, showcasing the methodology employed to achieve optimal accuracy through the fine-tuning of model parameters.

Performance Evaluation: Rigorous evaluation based on validation accuracy reveals the model's proficiency in accurately discerning and classifying image patterns, achieving an accuracy of 93.1% in epoch number 16. After that, a saturation in accuracy is shown after epoch number 20 as it is presented in Fig. 6.

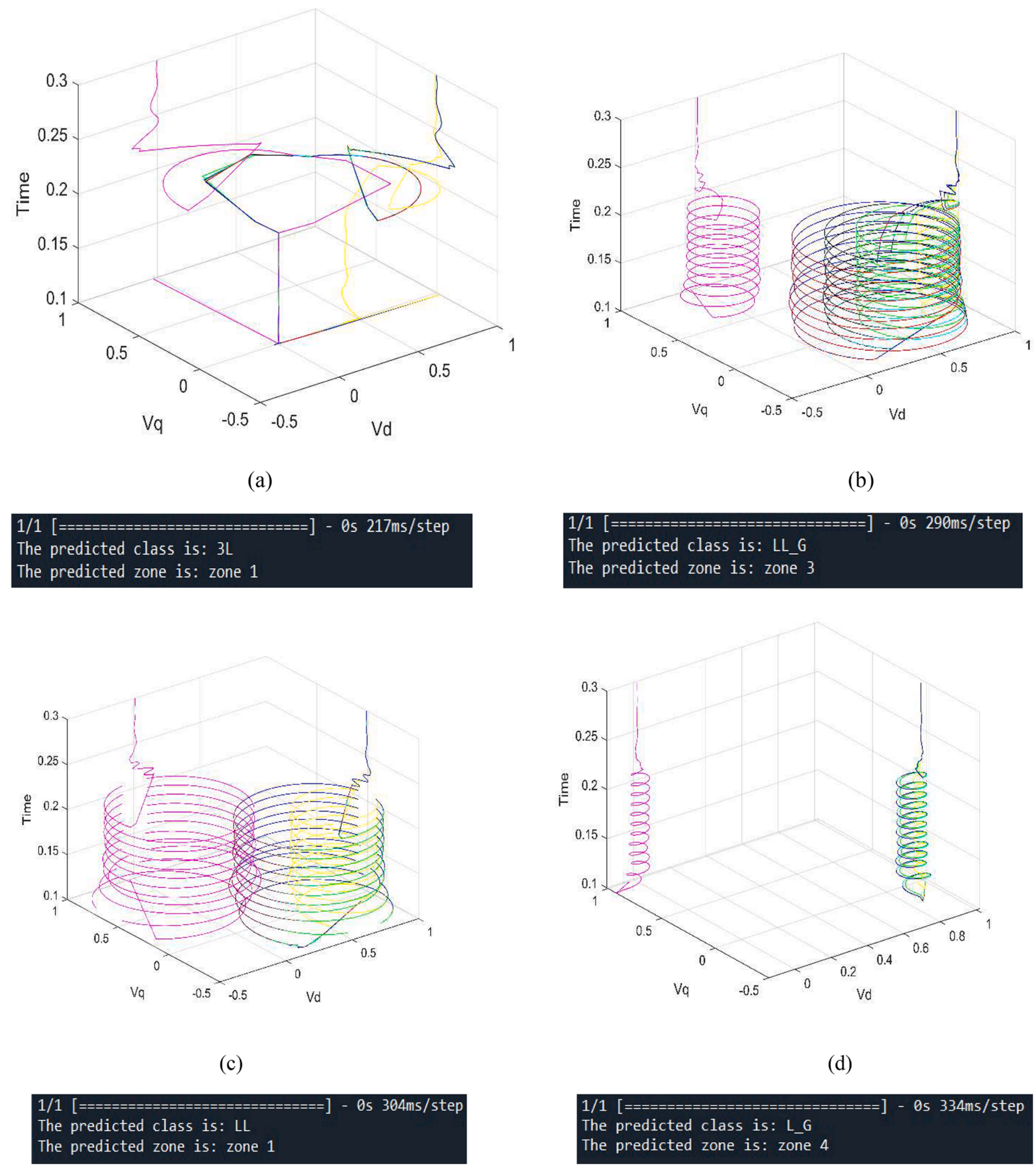

Fig. 7. Running the CNN model to predict new fault situation.
(a) The fault detected, fault type: 3 L, (fault resistance= 0.001 Ω),
(b) The fault detected, fault type: LLG, (fault resistance = 0.01 Ω)
(c) The fault detected, fault type: LL, (fault resistance = 0.1 Ω)
(d) The fault detected, fault type: LG, (fault resistance = 2 Ω).

The training and validation accuracy curves in Fig. 6 show fluctuations especially beyond 20 epochs, indicating that the model has reached a point of saturation. At this stage, further training does not significantly improve accuracy or reduce loss, suggesting the model has effectively captured the dataset's complexity and learned the underlying patterns. This phenomenon, characterized by diminishing returns, implies that the model is encountering its limit in generalizing further with the available parameters. Such fluctuations are typical when a model reaches its optimal learning capacity. Despite these variations, the model successfully distinguishes between healthy and faulty states and accurately identifies the type of fault, as shown in Fig. 7. Fig. 7a) is predicted as 3 L fault as the direct voltage decreases strongly, stays low and just rotates in medium/large arcs after the 3 L fault clears, while the quadrature voltage lowers significantly, stays low during the fault and arcs after fault clearing like in Fig. 5e). Fig. 7b) is predicted as LLG fault as, like in Fig. 5d), the direct voltage decreases significantly, then rotates in medium/large circles and does not reach the pre-fault value after the LLG fault, while the quadrature voltage decreases significantly, rotates in small to medium diameter circles and stays significantly lower than the pre-fault value. Fig. 7c) is predicted as LL fault, like in Fig. 5c), as the direct voltage decreases significantly, then rotates in large circles even intercepting and does not reach the pre-fault value after the LL fault, while the quadrature voltage decreases moderately, rotates in medium diameter circles and stays significantly lower than the pre-fault value. Fig. 7d) is alike Fig. 5b) and correctly predicted as LG fault, like in where the direct voltage decreases slightly, then rotates in small circles and nears the initial value after the LG fault, while the quadrature voltage decreases, rotates in small circles and stays lower than the pre-fault value.

The CNN is utilized to classify the type of fault based on high-

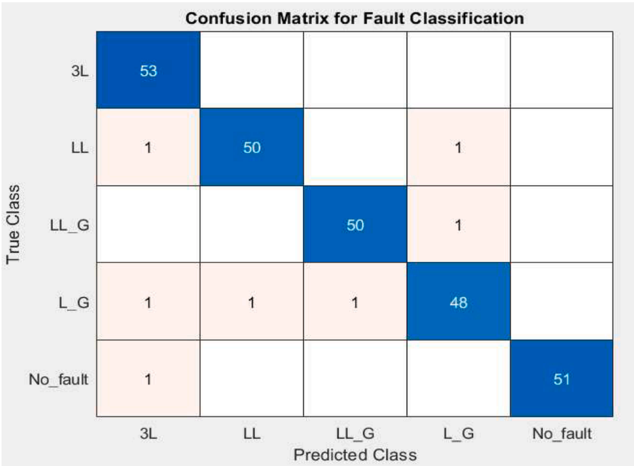

Fig. 8. The confusion matrix for fault classification.

resolution images derived from Park's vector transformation of the voltage waveforms. Once the fault type is determined, the PFPT algorithm is employed to identify the location (zone) of the fault. The PFPT algorithm processes the voltage amplitudes and uses a piecewise function to model the voltage behavior across different segments of the network, effectively reducing noise and highlighting the fault zone. By combining the classification capabilities of CNN with the precise localization provided by PFPT, this approach ensures both accurate fault identification and efficient fault zoning, thereby enhancing the reliability and response time of power distribution systems. The location of the faults is thus obtained using the PFPT algorithm.

The confusion matrix for the fault classification model is presented in Fig. 8. The model was evaluated on a validation set comprising 270 samples distributed across five fault categories: 3 L, LG, LL, LLG, and No-fault. The confusion matrix reveals that the model achieved an overall accuracy of 93.1%. Specifically, the model correctly classified 53 out of 54 samples for 3 L, 48 out of 51 samples for LG, 50 out of 52 samples for LL, 50 out of 51 samples for LLG, and 51 out of 52 samples for No_fault. Misclassifications occurred with the minimal rate (nearly 3% errors), indicating the accuracy of the model in distinguishing between different fault types.

7. Comparative analysis

Several advanced methods have been developed for fault location in distribution networks, utilizing techniques such as Convolutional Neural Networks (CNNs). These methods, while highly accurate, often require additional equipment and significant investment. The proposed method in this study utilizes existing data loggers installed at distribution substations, thus eliminating the need for additional equipment like Phasor Measurement Units (PMUs), etc. A comparative analysis between the proposed method and existing fault detection and feature extraction methods is presented in Table 6.

Most of these methods require special equipment like PMUs (Phasor Measurement Units), high-resolution data acquisition systems, and smart meters. The installation and maintenance of these devices at various points in the distribution network considerably increase expenses. For comprehensive network coverage, a large number of PMUs and smart meters are needed, each adding substantial costs for purchase, installation, and ongoing maintenance. These high-accuracy methods incur significant financial costs in large-scale networks.

In contrast, the proposed method valuates existing data loggers installed at distribution substations, making it a highly cost-effective and practical solution. By utilizing the existing infrastructure, this method minimizes the need for new investments and complex installations. It provides a competitive accuracy of 93.1%, offering a balance between cost and performance that is particularly beneficial for

Table 6
Fault detection and feature extraction methods compared.

Criterion	Proposed Method	Measurement-Based Methods	AI-Based Methods Using Park or Clarke Transformation	Impedance-Based Methods
Fault Types Detected	Single-line-to-ground, line-to-line, line-to-line-to-ground, and three-line faults	Faults in transmission lines [27], various faults in sustainable smart grids [29]	Open-circuit and short-circuit faults [24], faults in microgrids [26], power converter open-circuit faults [28], faults in distribution power lines [28]	Impedance measurement-related faults [30], faults detected using traveling waves [31]
Diagnostic Technique	CNN trained on images generated from voltage waveforms using Park's transformation	Reactive power measurements and wavelet transform [27], deep learning, and signal processing [29]	Current Park's Vector Pattern analysis [24, 25], Wavelet transformation combined with current Park's Vector approach [26], Neural networks with current Clarke-Concordia transformation [28]	DSP-based ellipse-fitting algorithm [30], traveling wave analysis [31]
Validation	Extensive simulation studies considering various fault resistances	Simulation and experimental validation [27], simulation and real-world data [29]	Simulation and laboratory tests [24], simulation and experimental validation [25, 26,28], experimental-based assessment [28]	Simulation and experimental validation [30,31]
Implementation Complexity	High (image processing and CNN training)	High (reactive power measurement and wavelet transform [27], deep learning model training and deployment [29])	Moderate to high (varies from current measurement and pattern recognition [24] to neural network training and transformation analysis [28])	Moderate (DSP-based implementation [30], traveling wave analysis [31])
Predictive Accuracy	High (93.1%)	Not explicitly quantified [3], relatively high (varies with model and data quality [6])	Not explicitly quantified, relatively high (varies with methods) [1,2,4,5],	Not explicitly quantified [30,31]
Advantages	Comprehensive fault detection\ Advanced machine learning techniques\Accurate fault prediction	Effective for various fault types in teed lines [27], Uses reactive power measurements for enhanced accuracy [27], Advanced deep learning techniques [29]	Effective for specific converter faults and simpler current measurement techniques [24], Uses current vector patterns [25], Combines wavelet transformation with Park's Vector [26], and accurate fault location [28]	Accurate impedance measurement and portable and low-cost solution [30], Effective fault location using traveling waves [31]
Applicable in Distribution Networks	Yes	Yes [27,29]	Limited (varies based on specific focus areas such as converters [24], power lines [26, 28])	Limited (focus on impedance measurements [30], traveling waves more applicable to transmission lines [31])
Need for Special Measurement Equipment	Data logger or Power Analyzer	Reactive power analyzers [27], high-performance computing hardware for deep learning [29]	Current transformers and data acquisition systems [24,25,26,28]	Impedance analyzers and DSP hardware [30], traveling wave detectors [31]

large-scale networks with numerous buses. This approach ensures effective fault detection and location without the financial and logistical burdens associated with deploying new equipment across the network.

8. Conclusions

This paper introduces a novel and efficient approach for instantaneous fault identification in medium voltage distribution networks using Park's transformation, noise reduction sine fitting algorithms, and convolutional neural networks. The proposed method showed versatility and effectiveness across various fault types, showcasing its potential for real-world automated fault detection, and characterization. Through simulation results, the paper establishes the capability of instantaneous voltage values at each bus to accurately identify fault conditions, emphasizing the practicality and reliability of the proposed diagnosis strategy.

The contribution of this study lies in the utilization of Park's transformation together with noise reduction sine fitting algorithms to simultaneously monitor faults in all system phases without the need to store previous waveform samples, addressing limitations present in existing fault location techniques. The distinctive feature of employing Park's transformation on voltage samples, rather than the commonly used current samples, sets this paper apart from previous works in the field. By employing the noise reduction sine fitting algorithm to generate Park vectors, the interpretability, and trustworthiness of the neural network-based fault detection system are enhanced, providing a valuable means of checking the results in real-world power system scenarios.

Additionally to the fault diagnosis strategy, the incorporation of CNNs for image classification adds a powerful dimension to the methodology. The CNN-based image classifier, labeled "sequential_64," proves effective in accurately discerning and classifying fault patterns, achieving an impressive validation accuracy of 93.1%. The model architecture, involving convolutional layers, batch normalization, and dropout layers, represents its capability to generalize effectively across diverse input variations.

This research presents a novel approach to identifying and characterizing faults in medium-voltage networks. The integration of CNN and PFPT allows for precise fault type classification and accurate fault zoning, enhancing the reliability and response time of power distribution systems.

Future work will address the prediction of the exact fault location at the bus level using the PFPT algorithm. It will focus on refining the fault detection and exact fault location down to the bus level by expanding the Convolutional Neural Network (CNN) architecture to distinguish fault types in each bus, providing precise bus-level localization. Increasing the complexity and diversity of training data, scaling up to larger distribution networks, evaluating how different distortion levels affect the performance of the (CNN), and incorporating additional electrical parameters can enhance the model's accuracy and applicability. Real-time implementation and integration into existing power distribution systems, along with collaboration with industry stakeholders for field trials, will validate the methodology's effectiveness in practical scenarios. Additionally, the challenges due to the integration of renewable energy sources into power systems can be considered to further enhance the system's robustness and adaptability [23].

Furthermore, incorporating power electronics components like UPFC and handling distributed generation and microgrids will be added to enhance the robustness of the CNN-based fault detection method [32]. These additions will allow for better adaptation to complex distribution systems with flexible power flow control and varying renewable energy sources, improving the fault detection accuracy and system adaptability.

Addressing these aspects in further work will contribute to advancing fault detection in medium voltage distribution networks and improving overall network effectiveness.

CRediT authorship contribution statement

Atefeh Pour Shafei: Software, Resources, Methodology, Investigation, Formal analysis, Data curation. **J.Fernando A. Silva:** Writing – review & editing, Supervision, Methodology, Investigation. **J. Monteiro:** Writing – review & editing, Validation, Supervision.

Declaration of competing interest

The authors declare the following financial interests/personal relationships which may be considered as potential competing interests: All authors declare that they have no conflicts of interest to disclose. If there are other authors, they declare that they have no known competing financial interests or personal relationships that could have appeared to influence the work reported in this paper.

Acknowledgments

This work was supported by national funds through FCT, Fundação para a Ciência e a Tecnologia, under project UIDB/50021/2020 (DOI:10.54499/UIDB/50021/2020).

Data availability

The authors do not have permission to share data.

References

[1] Ravi V. Ghodchar, Dr.R.G. Karandikar, Fault detection and classification in power transmission lines based on transient signal analysis: a review of different methodologies, International Journal of Engineering Research & Technology (IJERT) 02 (11) (2013) (11).
[2] Raheel Muzzammel, et al., Two Terminal Instantaneous Power-Based Fault Classification and Location Techniques for Transmission Lines, Sustainability. 15 (2023) 809, https://doi.org/10.3390/su15010809.
[3] I. Okakwu, P. Orukpe, E.A. Ogujor, Application of Superconducting Fault Current Limiter (SFCL) in Power systems: a Review, European Journal of Engineering Research and Science (2018).
[4] M. Hasan, S. Biswas, Md. Ali Azam Khan, Study of Switching Transient Over Voltage due to Transient Short Circuit Fault in a Power Distribution Network, in: International Conference on Robotics, Electrical and Signal Processing Techniques (ICREST), 2019.
[5] A. Raza, A. Benrabah, Th. Alquthami, M. Akmal, A Review of Fault Diagnosing Methods in Power Transmission Systems, MDPI journal, Appl. Sci. 10 (2020) 1312, https://doi.org/10.3390/app10041312.
[6] F.V. Lopes, D. Fernandes Jr., W.L.A. Neves, A Traveling-Wave Detection Method Based on Park's Transformation for Fault Locators, IEEE Transactions on Power Delivery 28 (3) (2013) (7).
[7] P. Gale, P. Crossley, X. Bingyin, G. Yaozhong, B. Cory, J. Barker, Fault location based on traveling waves, in: Proc. 5th Int. Conf. Develop. Power Syst. Protect, 1993, pp. 54–59.
[8] A.C. Adewole, R. Tzoneva, Sh. Behardien, et al., Distribution network fault section identification and fault location using wavelet entropy and neural networks, Elsevier, Appl. Soft. Comput. 46 (09) (2016) 296–306.
[9] M. Azeroual, Y. Boujoudar, et al., A multi-agent-based for fault location in distribution networks with wind power generator, Wind Engineering: The International Journal of Wind Power (2021).
[10] D. Shu, Zhou Zhenyu, Zhu Ke, A Synchronous Distributed Generator Excitation Control Measures Aimed at Automatic Reclosing, in: IEEE Second International Conference on Power, Electronics and Computer Applications (ICPECA), 2022.
[11] M. Majidi, A. Arabali, M. Etezadi-Amoli, Fault Location in Distribution Networks by Compressive Sensing, IEEE Transactions on Power Delivery (2015).
[12] Gargi Bag, Linus: challenges and opportunities of 5G in power grids, in: 24th International Conference on Electricity Distribution, Glasgow, 2017.
[13] N. Okpura, E. Okafor, K.M. Udofia, Comparative Analysis of Fuzzy Inference System (FIS) And Adaptive Neuro-Fuzzy Inference System (ANFIS) Methods in the Classification and Location of High Impedance Faults on Distribution System, European Journal of Engineering and Technology Research (2020).
[14] A.García E.Personal, A. Parejo, D. Larios, F. Biscarri, C. León, A Comparison of Impedance-Based Fault Location Methods for Power Underground Distribution Systems, Energies. (Basel) (2016) 1022, https://doi.org/10.3390/en9121022.
[15] C.J. O'Rourke, M.M. Qasim, M.R. Overlin, J. Kirtley, A Geometric Interpretation of Reference Frames and Transformations: dq0, Clarke, and Park, IEEE transactions on energy conversion (2019).
[16] Kh.O. Mokhtar, M. Boudiaf, L. Cherroun, Fault Diagnosis of Power Transmission Using Park's Method, in: 19th International Multi-Conference on Systems, Signals & Devices (SSD'22), 2022.

[17] C. Lin, et al., Fault Detection, Classification and Localization Along the Power Grid Line Using Optimized Machine Learning Algorithms, International Journal of Computational Intelligence Systems (2021).

[18] D. Mondal, A. Chakrabarti, A. Sengupta, Power System Small Signal Stability Analysis and Control, 2nd Edition, 2020. ISBN 978-0-12-817768-6.

[19] P.M. Ramos, A.Cruz Serra, A new sine-fitting algorithm for accurate amplitude and phase measurements in two-channel acquisition system, Elsevier Measurement Journal 41 (2) (2008) 135–143 (2).

[20] Ch.Rothleitner Sh.Lin, N. Rogge, Amplitude estimation using three-parameter sine fitting algorithm in the Planck-Balance, in: 23rd IMEKO TC4 International Symposium Electrical & Electronic Measurements Promote Industry 4.0 September 17-20, 2019.

[21] Y. Huang, R. Wu, P. Ou, A Fully Sequential Methodology for Convolutional Neural Networks, Published in arXiv.org 27, Computer Science 11 (2018).

[22] M. Marinov, I.Valova Y.Kalmukov, Impact of image resolution on the search accuracy and results ordering, in: 2021 International Conference Automatics and Informatics (ICAI) 15, Date Added to IEEE Xplore, 2021.

[23] A Single-Pole Filter-Assisted Improved Protection Scheme for the TCSC Compensated Transmission Line Connecting Large-Scale Wind Farms, IEEE Journal of Emerging and Selected Topics in Industrial Electronics 5 (2) (2023) 346–358, https://doi.org/10.1109/JESTIE.2023.3345791 (22)(12).

[24] M.M. Saha, J. Izykowski, E. Rosolowski, Fault Location on Power Networks, Springer, 2009.

[25] P. Gale, et al., Fault location based on traveling waves, in: 5th Int. Conf. Develop. Power Syst. Protect, 1993.

[26] E. Personal, et al., A Comparison of Impedance-Based Fault Location Methods for Power Underground Distribution Systems, Energies. (Basel) 9 (12) (2016) 1022.

[27] F.V. Lopes, et al., A Traveling-Wave Detection Method Based on Park's Transformation for Fault Locators, IEEE Transactions on Power Delivery 28 (3) (2013).

[28] N. Okpura, et al., Comparative Analysis of Fuzzy Inference System (FIS) And Adaptive Neuro-Fuzzy Inference System (ANFIS) Methods in the Classification and Location of High Impedance Faults on Distribution System, European Journal of Engineering and Technology Research (2020).

[29] A.C. Adewole, et al., Distribution network fault section identification and fault location using wavelet entropy and neural networks, Elsevier Applied Soft Computing 46 (2016) 296–306.

[30] S. Wei, X. Zhang, Y. Xu, Y. Fu, Z. Ren, F. Li, Extended Park's vector method in early inter-turn short circuit fault detection for the stator windings of offshore wind doubly-fed induction generators, IET Gener. Transm. Distrib. vol. 14 (2020) 3905–3912.

[31] M. Messaoudi, A. Flah, A.A. Alotaibi, A. Althobaiti, L. Sbita, C.Z. El-Bayeh, Diagnosis and fault detection of rotor bars in squirrel cage induction motors using combined Park's vector and extended Park's vector approaches, Electronics. (Basel) 11 (2022) 380.

[32] S. Biswas, P. Kumar Nayak, B. Ketan Panigrahi, G. Pradhan, An intelligent fault detection and classification technique based on variational mode decomposition-CNN for transmission lines installed with UPFC and wind farm, Elsevier Journal on Electric Power Systems Research 223 (10) (2023) 109526.

Atefeh Pour Shafei's Biography: My name is Atefeh Pour Shafei, and I am from Iran. I hold a master's degree in Electrical Engineering.

Enrolling in the Electrical Engineering undergraduate program at Bu-Ali Sina University in 2001 with a GPA of 16.07, followed by admission to a master's degree program in the same field at Shahid Chamran University with a GPA of 17.91, were the key milestones in my academic journey toward achieving my goals regarding power system investigations.

My academic studies led to exciting opportunities to work as a technical expert for various power distribution companies. My focused pursuit to enhance my practical skills and achieve my career objectives in distribution networks began when I was involved in the position of head of the GIS department and then as a senior expert in operation monitoring and network fault analysis at the Tehran Electric Power Distribution Company since 2017. During these years, I carried out numerous investigations on optimization techniques, the study of the Harmonic Behavior of different loads, the advantages of using photovoltaic energy, as well as the identification of harmonics in electrical systems through the wavelet transform.

My awards include:

☐ The top Researcher of Shahid Chamran University of Ahvaz, 2009.

☐ The first-best student in the master's degree of Shahid Chamran University of Ahvaz, 2009

☐ Elite Approval from Tavanir Company (Tavanir is responsible for the Management of Generation, Transmission, and Distribution of Electric Power in Iran)

☐ The top researcher of Tehran Electric Power Distribution Company: 2019 and 2021

I am planning to register for the IST PhD program in 2024 and intend to pursue my PhD at Lisbon University under the supervision of Professor Jose Fernando Alves da Silva and Professor Joaquim Monteiro.

My scientific interests include:

☐ Cutting-edge applications of artificial intelligence in the sustainable development of smart renewable systems and distribution networks.

☐ Utilizing renewable forms of energy to mitigate global warming.

☐ Network fault analysis and providing corrective suggestions.

☐ Load estimation in distribution network